Effect of monomer concentration and functionality on electro-optical properties of polymer-stabilised optically isotropic liquid crystals

Ramesh Manda, Srinivas Pagidi, MinSu Kim, Chul Ho Park, Hye Sun Yoo, Kaur Sandeep, Young Jin Lim & Seung Hee Lee

Published online: 27 Sep 2017.

Submit your article to this journal

View related articles

View Crossmark data

Taylor & Francis
Taylor & Francis Group

Check for updates

Effect of monomer concentration and functionality on electro-optical properties of polymer-stabilised optically isotropic liquid crystals

Ramesh Manda [a], Srinivas Pagidi[a], MinSu Kim[b], Chul Ho Park[a], Hye Sun Yoo[a], Kaur Sandeep[a], Young Jin Lim[a] and Seung Hee Lee[a]

aApplied Materials Institute for BIN Convergence, Department of BIN Convergence Technology and Department of Polymer-Nano Science and Technology, Chonbuk National University, Jeonju, Republic of Korea; bDepartment of Physics and Astronomy, Johns Hopkins University, Baltimore, MD USA

ABSTRACT

Optically isotropic nature can open a new type of high-performance liquid crystal (LC) displays. The main features emerge from the interaction between LC and polymer network at the interface. At this point, we investigated the influence of cross-linking monomer concentration and functionality on electro-optic properties of optically isotropic liquid crystal (OILC) obtained by polymerisation-induced phase separation method. Interestingly, we obtained a pore-like network structure constructed by highly interlinked polymer beads in acrylate monomers and achieved fast decay response time (0.6 ms). We found that the voltage-dependent hysteresis was mostly eliminated (~0.25%), and the contrast ratio was enhanced (1:1550) for high functional monomers. The result inspires a simple way to optimise the materials to fabricate a high-performance OILC device and it shows high-transparency, low-driving voltage, hysteresis-free and sub-millisecond response time.
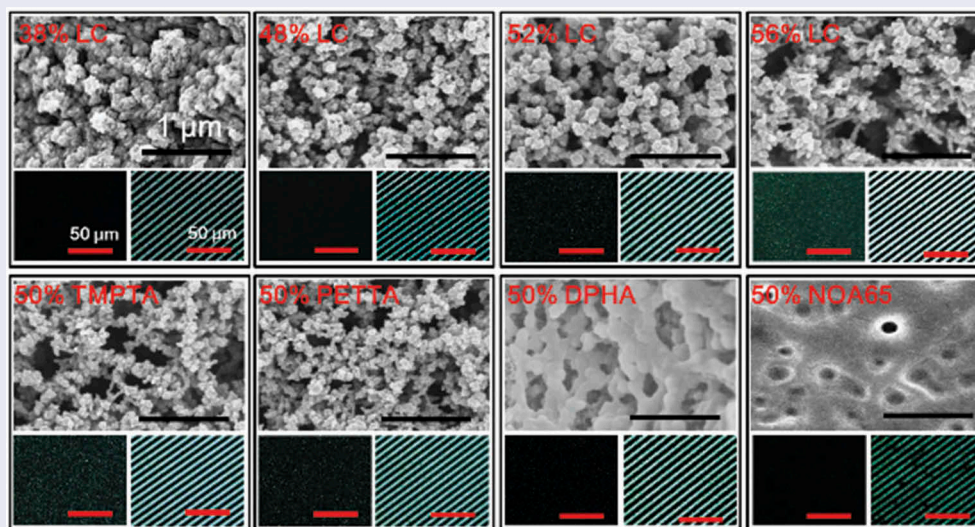
1. Introduction

Liquid crystal (LC) display technology has achieved a tremendous growth in flat panel displays owing to its compact size and minimal power consumption. Among various LC technologies, an optically isotropic liquid crystal (OILC) mode shows the manufacturing advantages (alignment layer free, cell gap insensitivity and low cost due to minimal manufacturing steps) and novel display properties (fast response, high contrast ratio, touchmura free, wide viewing angle due to optically isotropic state and adaptability to flexible devices), which would make the mode a potential candidate for future displays [1–6]. The polymer-stabilised blue-phase liquid crystal (PSBPLC) is one example of OILC such that its prototype was already demonstrated [7]. Although most of the advantages of PS-BPLC are quite similar to that of OILC, shortcomings remained for PS-BPLC such as its high driving voltage, electro-optical hysteresis, narrow temperature range to polymer-stabilisation and temperature-

dependent Kerr constant. Also, the optical activity of PS-BPLC limits the optically isotropic nature as a quasiisotropic state [8]; the electro-optic property is dominated by electrostriction forces when applied electric field exceeds the critical field [9], and thus, the residual birefringence limits the contrast ratio [10]. Considering demerits of PSBPLC, the OILC obtained by polymerisation-induced phase separation (PIPS) could be a more promising way to realise high-performance displays. Unlike PSBPLC, the OILC phase obtained by PIPS method, the electro-optical properties are independent of operation temperature, and high thermal stability could be easily achieved [11–14].

In PIPS method, the small LC droplets, typically below 300 nm, are formed in a polymer network [15]. Usually, the low-molecular-weight reactive monomers mixed with a LC. When a monomer is polymerised, the phase separation usually occurs by monomer nucleation and growth, thereby the LC molecules are formed as a droplet separated by network walls [16]. The droplets randomly distribute in the polymer matrix and the optically isotropic property can be realised when a visible light passes through this phase. Under an external field, LC molecules reorient along the field direction; therefore, it induces birefringence along the field direction.

Considering the close interaction between the polymer network and LC molecules in OILC phase, the driving field drastically increases that is opposite to the requirement of real devices. Generally, the required driving voltage is higher than 50 V_{rms} to achieve 2π phase shift in a 10-µm cell. Employing high dielectric constant LC is the straightforward way to solve this problem, but it leads to slow capacitor charging when addressed to thin film transistor and increases the rotational viscosity which is not desirable for fast response. Another major challenge in this system is to minimise the scattering which improves the isotropic nature and contrast ratio while maintaining the efficient electro-optic properties. Many trails have been made to overcome this problem such as encapsulation, doping star polymer and improving the driving scheme [17–19]. However, making better OILC phase with high LC concentration is still remaining as a critical issue. Moreover, the other electro-optical properties such as response time, hysteresis and contrast ratio are highly dependent on the LC molecules interaction at network interface and droplet size, shape and distribution [20–24]. Although the rise time has been improved by introducing overdriving technique, the decay time still remains a major challenge. To overcome the

aforementioned challenges, the novel cross-linking monomers need to be adopted and the concentration and functionality are required to be finely tuned. Numerous trails have been done to improve the driving voltage, hysteresis free, fast response and fabrication techniques of OILC films based on PIPS method [4,25–30]. To make an efficient OILC device, the effect of cross-linking monomer concentration and functionality should be studied in detail.

In this report, we systematically investigated the impact of cross-linking monomer concentration and functionality on electro-optical properties of OILC. Interestingly, we obtained the pore-like network structure constructed by highly interlinked polymer beads in acrylate monomers. We found this system is free of hysteresis (~0.25%), and high contrast ratio (1:1550) while keeping fast decay response time (0.6 ms). This work would give a simple way to find optimised condition of pre-polymers in an OILC mixture, which is strongly desirable for displays and photonic application.

2. Theory

The driving principle of the OILC film is schematically shown in Figure 1. After phase separation, sub-micron-sized LC domains form in polymer network and directions of LC molecules at polymer surfaces are random. When visible light passes through the cell and the correlation length of the polymer network is shorter than the wavelength of the light, the LC/polymer matrix is optically isotropic and there is no light scattering because the LC director is randomly oriented. With the optical set-up with the film placed in between crossed polarisers, the incident light passes through it without any phase change and blocked by the second polariser. Thus, it appears dark and it is schematically represented in Figure 1(a). Under an applied field, the LC directors are reoriented along the field direction and birefringence is induced. Thus, it results in a bright state as shown in Figure 1(b).

According to the scattering theories, the light scattering occurs due to change in the refractive index of the medium on the light path. When the size of LC droplets in a polymer matrix is assumed to be similar, the fraction of scattered light to the light incidence can be described as $B = N\sigma_{avg}d$, where N, σ_{avg} and d denote number density of droplets, average backscattered cross-section of droplets and the distance of the light travelling, respectively. Assuming the radius of a single droplet is smaller than the wavelength in the Rayleigh–Gans limitation and the angle between the direction of incident light and backscattered light is
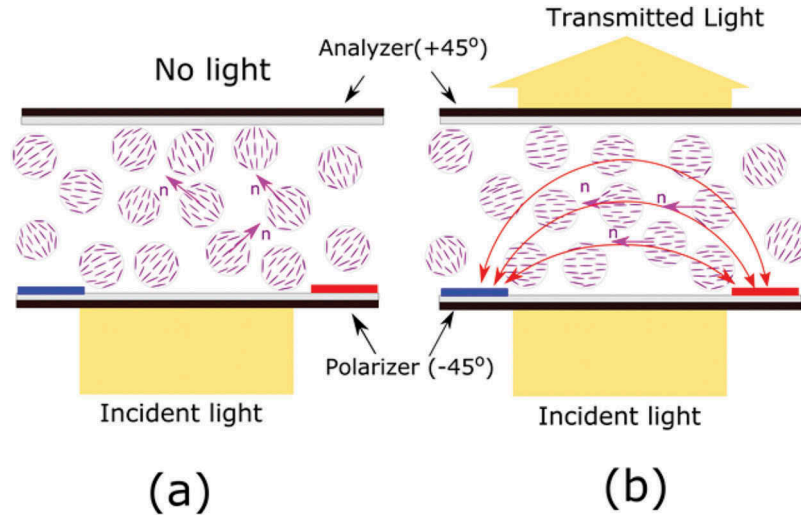
Figure 1. (Colour online) Schematic representation of OILC switching under crossed polarisers. (a) At zero-field and (b) at the driving field. The arrows represent the individual droplet's average orientation. The blue and red colours represent a signal and common electrodes, respectively.

assumed to be very small, the backscattered light can be described as [31],

$$\sigma_{avg} \propto |m - 1|^2 k^4 R^6, \quad (1)$$

where R is the radius of droplets; k is wave vector ($2\pi n_p/\lambda$, n_p = refractive index of the polymer matrix) and $m = n_{LC}/n_p$ is the ratio of the refractive index of LC to the polymer matrix.

The birefringence of OILC under an electric field is induced as the induced birefringence $\Delta n_{ind} = K\lambda E^2$, where K is Kerr constant, Δn_{ind} is induced birefringence, λ is the wavelength of the incident light and E is an applied electric field. The induced birefringence at higher field is more precisely explained by the extended Kerr effect, which can be described as [32,33]

$$\Delta n_{ind} = \Delta n_s \left\{ 1 - \exp\left[-\left(\frac{E}{E_s}\right)^2 \right] \right\}, \quad (2)$$

where Δn_s is saturated birefringence and E_s is saturated applied electric field. When an applied electric field (E) gets close to E_s, the Δn_{ind} reaches Δn_s. Here, it is worth to describe the Kerr constant (K) [6],

$$K = \frac{1}{15} \Delta n \Delta \varepsilon \varepsilon_o \left(\frac{R}{\lambda W_s}\right), \quad (3)$$

where W_s is surface anchoring energy for the reorientation of LC director and $\Delta\varepsilon$ is dielectric anisotropy of the LC. Unlick other optical isotropic materials, the OILC phase obtained by PIPS method is highly affected by surface anchoring energy.

3. Experiments

To prepare an OILC films, we mixed high dielectric constant nematic LC with different photo curable cross-linkers. We used MLC2053 ($\Delta\varepsilon$ = 42.6, Δn = 0.235 at 589.3 nm, T_{NI} = 86°C, from Merck Advanced Technology in Korea) as a nematic LC and four acrylate monomers, namely, DPHA (dipentaery-thritol penta-/hexa-acrylate, n_p = 1.483, Sigma-Aldrich), PETTA (pentaerythritol tetraacrylate, n_p = 1.487, Sigma-Aldrich), TMPTA (trimethylolpro-pane triacrylate, n_p = 1.474, Sigma-Aldrich) and EHA (2-ethylhexyl acrylate, n_p = 1.436, Sigma-Aldrich), where n_p is refractive index of the isotropic polymer. We also employed one thiol-ene-based optical adhesive NOA65 (Norland Optical Adhesive, n_p = 1.524, from Norland Products Inc., USA). The schematic molecular structure of each monomer is shown in Figure 2. A small amount of the radical rich photo-initiator, Irgacure 907 (from Merck Advanced Technology, Korea), was added to initiate the radical photo poly-merisation. Here, we intentionally used mono-acrylate monomer, EHA, aimed to decrease the viscosity of the high functionalised monomers and consistent material concentrations used in this report are shown in Table 1. All these materials are used without further purification. To investigate both the critical monomer concentration and monomer functionality effect on electro-optical properties, we employed increase in monomer concentrations in one set of samples with equal monomer ratios, S1–S4, and manipulated mono-mer functionality on another set of samples, S5–S8.
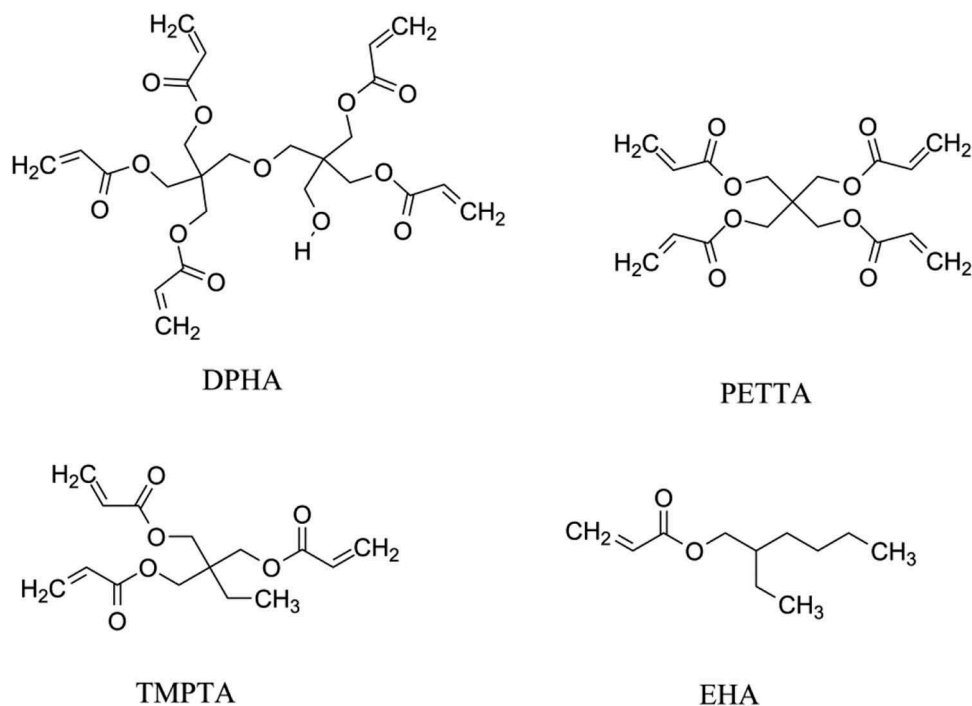
Figure 2. Molecular structures of reactive monomers used in this work.

Table 1. LC and monomer concentrations used for preparing the OILC film.

Sample	MLC2053 (wt.%)	TMPTA (wt.%)	PETTA (wt.%)	EHA (wt.%)
S1	38	30	30	2
S2	48	25	25	2
S3	52	23	23	2
S4	56	21	21	2
S5	50	48	-	2
S6	50	–	48	2
S7	50	48[a]	–	2
S8	50	50[b]	–	–

[a]DPHA used as monomer.
[b]NOA65 used as monomer.

Polarising optical microscopy (POM) was used to observe an optically isotropic phase using a polarising optical microscope (Nikon eclipse E600 POL) with a CCD camera (Nikon, DXM 1200). The wavelength-dependent transmittance measured with UV-Visible spectroscopy (SCINCO, S-3100) from ultraviolet to near-infrared region. The digital camera (Samsung, NX1000) used to take the cell photographic images. All the electro-optical properties such as driving field, electro-optic hysteresis and response time of obtained films were measured from voltage-dependent transmittance curves. The cells were placed between the crossed polarisers in such a way that the long-side electrode direction is 45° to the polarisers, and transmittance is detected by a photo-detector and signal read by an oscilloscope (Tektronix, DPO2024B) using a He-Ne light source (λ = 633 nm) while applying square wave by a function generator (Tektronix, AFG3101C) and amplifier (FLC A400). The efficiency of the dark state was calculated from the off-state POM images by using an image analyser i-solution^{TM} (iM Technology, i-Solution Inc.). Next, we experimentally evaluated the polymer effect on contrast ratio and light leakage with crossed polarisers. The contrast ratio was measured by detecting both on-state and off-state light transmittances using a white light source that pass through normal to the cell substrate. The light leakage defined as amount of light leaking out under crossed polarisers when applied filed is zero. Finally, the obtained polymer network structures was examined by field emission scanning electron microscopy (FESEM).

We employed an IPS (in-plane switching) cell having a periodic comb-like indium tin oxide (ITO)-coated electrodes on the bottom substrate with no electrode on the top substrate. The long and uniformly shaped electrodes are separated by 4-μm spacing and each electrode width is 4 μm. The separation between the two glass substrates was fixed to 10 μm with uniformly shaped silicon ball spacers. The homogeneous OILC mixture is filled in the IPS cells by capillary action at a temperature greater than the clearing temperature of the nematic LC, 90°C. Finally, the phase separation process was initiated by exposing 350 mW/cm^2 intensity of 365 nm UV light for 10 min at isotropic phase, 90°C.

4. Results and discussion

The wavelength-dependent transmittance was measured by UV-visible spectroscopy from ultraviolet to near-infrared region after phase separation, and the obtained transmission spectra are shown in Figure 3(a). Unpolarised light source with a wavelength range from 200 to 1100 nm is used. No polarisers were employed here. The relative transmittance change is more pronounced in the visible range, but it is not profound in the near-infrared region. Measured transmittance varies from 77% to 89% depending on the monomer concentration and functionality. The transmittance is affected by both the monomer functionality and concentration. We have also observed the transparency of cells by taking photographic images, as shown in Figure 3(b). The background characters are unclear for S4 and S5 due to light scattering from the film. The photographic images seem to indicate that the transparency of final obtained film is proportional to monomer concentration. The background images clearly appear with high monomer concentration samples and high functionalised monomer samples. Therefore, the scattering free OILC can be achieved by the high functionalised and high concentration of crosslinking monomers.

We measured the electric field-dependent transmittance of prepared samples as shown in Figure 4(a). The threshold electric field (E_{th}) and driving electric field (E_{op}) are defined at 10% and 90% transmittance, respectively. The hysteresis is defined as the voltage difference between the ascending and descending field sweeps at 50% transmittance. The rise time (τ_{rise}) and decay times (τ_{decay}) are defined as the time taken for 10–90% transmittance change when the sample is driven to its peak transmittance and transmittance change from 90% to 10% when applied field is zero, respectively. In other words, the rise time is defined as reorientation of LC director from random order to field direction that is strongly influenced by applied field, while the decay time defined as the nematic director relaxation to equilibrium position after the field is withdrawn which is independent of the applied field.

Figure 4(a) shows that the transmittance starts to increase with applied field, i.e., the sub-micron-sized droplets tend to reorient along the electric field direction resulting in induced birefringence, following Equation (1). On the other hand, the highest saturation transmittance implies that the induced birefringence (Δn_{ind}) saturates, as indicated by Equation (2). The measured E_{op} are 13.5, 11.5, 9, 7.5, 8.1, 9.2, 12 and 7.5 $V_{rms}/\mu m$ for S1–S8, respectively. The measured E_{th} are 1.9, 1.7, 1.2, 0.8, 1.6, 1.6, 1.8 and 0.6 $V_{rms}/\mu m$ for S1–S8, respectively. Both E_{th} and E_{op} decrease by decrease in monomer concentration as from S1 to S4. It could be due to linear dependence of Kerr constant on LC concentration. From S5 to S7, the increase in E_{th} and E_{op} could be due to change in droplet size and anchoring energy at interface (Equation (3)). The transmittance curves of S4, S5 and S6 samples deviate from baseline, probably due to scattering effect. Although the E_{th} and E_{op} are low for S4 and S5, the strong scattering effect makes them pseudo-OILC. Therefore, highly functional and high concentration monomers are the best choices to make an OILC.
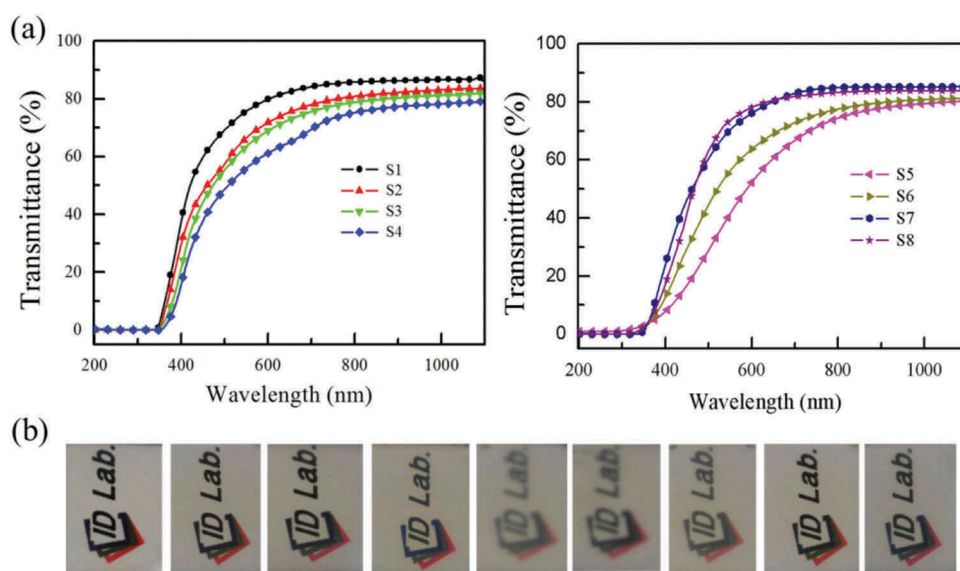

Figure 3. (Colour online) (a) UV-Vis transmission spectra of prepared OILC samples after phase separation. (b) The photograph image of prepared cells. Photos have been taken at ambient light conditions and a uniform height was maintained to observe the backscattered effect from the background surface.
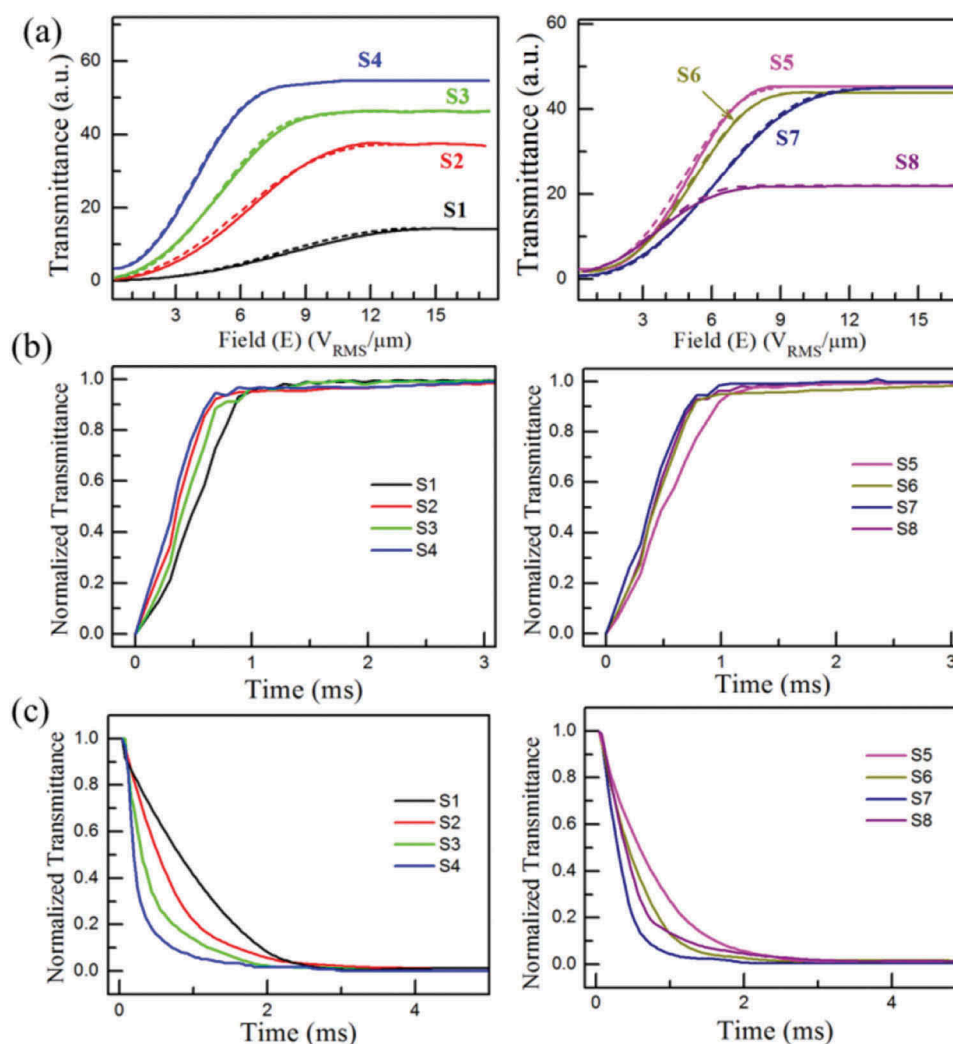
Figure 4. (Colour online) Measured electro-optic properties of prepared OILC samples under crossed polarisers: (a) field-responsive transmittance in which the solid and dashed lines represent field increasing and decreasing voltage swipes, respectively. (b) Rise response time. (c) Decay response time.

We also measured the percentage of electro-optical hysteresis from voltage-dependent transmittance curves. The measured hysteresis is 4.2%, 2.4%, 1.1%, 0.8%, 2.2%, 0.96%, 0.25% and 1.2% for samples from S1 to S8, respectively. Here, we would assume that the hysteresis is strongly affected by monomer network morphology such as droplet shape, size, uniformity, etc. The hysteresis reduced dramatically up to about 0.25% for S7. It could be due to the strongly anchored LC molecules to polymer network. In Figure 4(b,c), the rise time is mostly not affected by the polymer concentration and functionality whereas both strongly affected the decay time. The sample S7 shows the fastest decay time (0.6 ms) and the obtained value is faster than the result in reference [4]. The hysteresis-free and fast response time could be due to stronger anchoring at the polymer network.

For better understanding of the obtained OILC, we observed the phase under crossed polarisers using POM. The phase appeared black, revealing that the incident light passes through the film and then blocked by the second polariser. No change in transmittance is observed when the sample is rotated on the stage. Hence, the obtained film is optically isotropic, as illustrated in Figure 5. From obtained POM images, one can notice that the light leakage at field-off state is increasing with the decreasing monomer concentration, S1–S4. The excellent dark state is achieved for high monomer concentration samples. We measured the efficiency of dark state at off-state with i-solution software in which the zero dark level is predefined. The measured dark levels are 2.9, 9.3, 17.2, 42.9, 39.5, 25.3, 3.0 and 2.9 for samples from S1 to S8, respectively. The functionality of the monomer also strongly influences
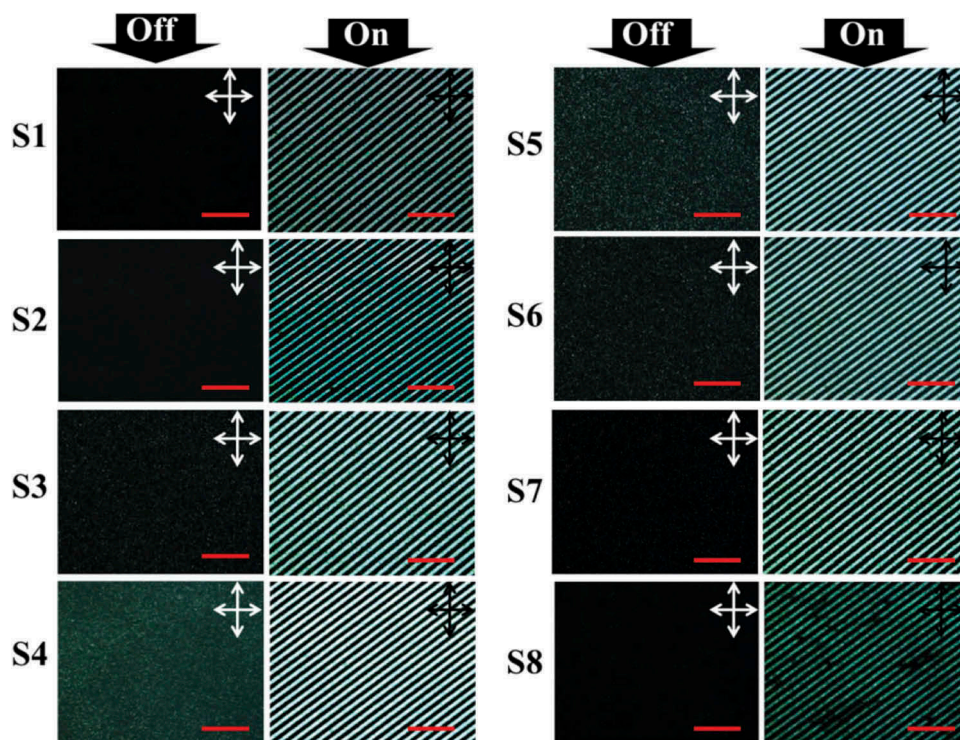
Figure 5. (Colour online) POM images of the obtained OILC film under crossed polarisers. The first column represents texture at the field off-state and next column represents textures when driven to square wave field. Scale bar represents 50 μm. The long-side ITO electrode was set to 45° to the polariser.

the dark level at off-state. In addition, the on-state transmittance was also strongly influenced by both the monomer concentration and functionality. For a better understanding of on-state and off-state transmittances, we measured light leakage and contrast ratio.

In Figure 6, we explore the polymer functionality and concentration effect on contrast ratio and light leakage with crossed polarisers. The contrast ratio is defined as the ratio between maximum transmittance (field-on), and minimum transmittance (field-off) by using visible light that propagates normal to the substrate. The light leakage is defined as the amount of light leaking out through the crossed polarisers when applied field is zero. We compared the results with well-studied NOA65 because the contrast ratio highly depends on the experimental conditions such as nature
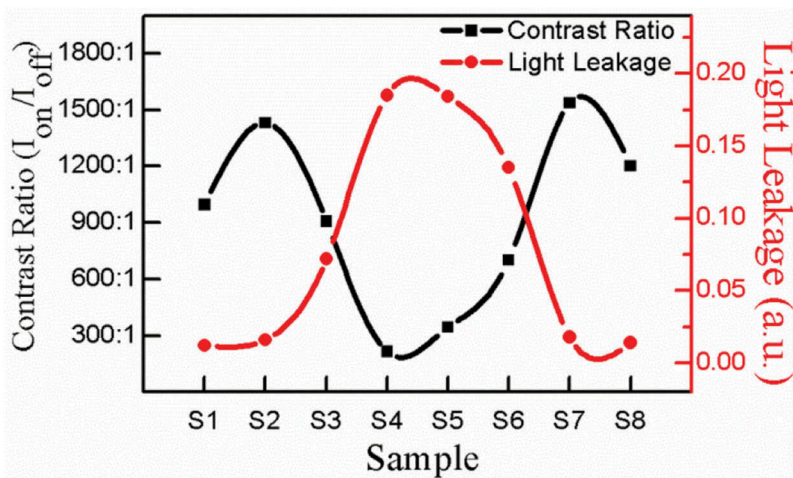

Figure 6. (Colour online) The contrast ratio and light leakage of prepared OILC films under crossed polarisers at normal direction. The contrast ratio is defined as the ratio of maximum and minimum transmittance when the cell is driven with the driving voltage and zero voltage, respectively. The light leakage was defined as the amount of light leaking out through crossed polarisers when applied field is zero.

of the light source, the acceptance angle of the detector, polariser thickness and efficiency, and alignment of polarisers. In Figure 6, the off-state light leakage mostly eliminated for high monomer concentration samples (S1, S2 and S3) and high functional monomer samples (S7 and S8). The contrast ratio enhanced for high concentration and high functionality monomers. The highest contrast ratio 1:1550 is achieved for S7. The off-state light leakage and contrast ratio are inversely proportional to each another. The minimum light leakage at off-state was a crucial parameter for improving the contrast ratio.

Finally, the network structure was examined by FESEM. The LC molecules were extracted from the film by immersing it in hexane for approximately 48 h. After LC molecules were extracted, the two substrates were taken apart carefully. Finally, the surface of the polymer film was sputtered with gold and microstructure was observed normal to the substrate; no tilt of the substrate was performed. From Figure 7, it is clear that the pore-like polymer network constructed by highly interlinked polymer beads was achieved in acrylate monomers in S1–S7 while highly spherical and isolated droplets are formed in thiol-ene based

monomers in S8. The pore size was increasing with decrease in both monomer functionality and concentration. The filling factor of LC and pore size is measured with ImageJ software, a Java-based image-processing program developed at the National Institutes of Health and the measured filling factors of LC are 15%, 24%, 28%, 31%, 30%, 29%, 32% and 19% for S1, S2, S3, S4, S5, S6, S7 and S8, respectively. It is clear that some of the pores, in S4 and S5, are larger than 300 nm and those can affect the propagation of the incident light by scattering. The close observation of pore shape suggests that the elongated pores were formed in acrylate monomers. A smaller and elongated shape would make strong coupling interaction of LC molecules at polymer interface, which could be the reason for reduced hysteresis and fast decay time. The surface of the polymer strand is smoother for S7 and filling factor is higher, which could be the reason for high contrast ratio and fast decay time.

5. Conclusion

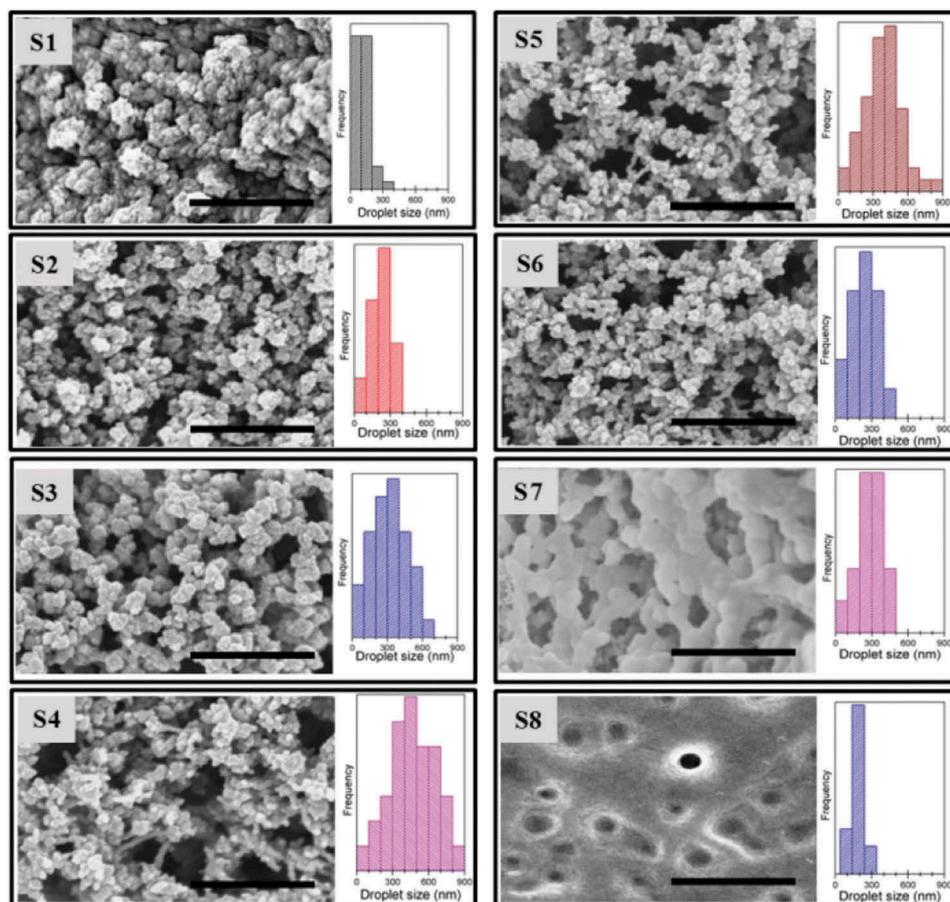We have examined the performance of OILC system as a function of cross-linking monomer concentration

Figure 7. (Colour online) Polymer network morphology of prepared OILC film obtained from FESEM. The scale bar is equal to 1 μm.

and functionality. We obtained a hysteresis-free and fast-response OILC phase. Interestingly, we obtained a highly inter-linked pore-like polymer network constructed by highly interlinked polymer beads in acrylate monomers. The evolution of polymer network architecture revealed that high functional polymers formed smaller LC droplets and enhanced the coupling interaction between LC molecules and polymer walls. It leads to reduce the hysteresis (0.25%) and high contrast ratio (1:1550) while keeping fast decay response time as 0.6 ms. This work highlights the cross-linking monomer concentration and functionality effect on switching performance and it suggests a simple way to optimise the consistent materials for potential applications. These OILC films can improve the performance of displays by increasing the accuracy of grey scale, such that it can have less sensitivity to hysteresis, less image motion blur due to fast response time and high contrast ratio. Also, it can be a promising material for the flexible display application.

Acknowledgements

Disclosure statement

No potential conflict of interest was reported by the authors.

ORCID

Ramesh Manda 🔴 http://orcid.org/0000-0002-6171-7991

References

[1] Kim MS, Lim YJ, Yoon S, et al. A controllable viewing angle LCD with an optically isotropic liquid crystal. J Phys D: Appl Phys. 2010;43:145502.
[2] Choi SW, Yamamoto SI, Iwata T, et al. Optically isotropic liquid crystal composite incorporating in-plane electric field geometry. J Phys D: Appl Phys. 2009;42:112002.
[3] Bahadur B. Liquid crystals: applications and uses. Singapore: Singapore World Scientific (Vol. 1); 1990.
[4] Park NH, Noh SC, Nayek P, et al. Optically isotropic liquid crystal mixtures and their application to high-performance liquid crystal devices. Liq Cryst. 2015;42:530–536.
[5] Rao L, Ge Z, Wu ST, et al. Low voltage blue-phase liquid crystal displays. Appl Phys Lett. 2009;95:231101.
[6] Yang YC, Yang DK. Electro-optic Kerr effect in polymer-stabilized isotropic liquid crystals. Appl Phys Lett. 2011;98:023502.
[7] Lee H, Park HJ, Kwon OJ, et al. The world's first blue phase liquid crystal display. SID Int Symp Dig Tech Pap. 2011;42:121–124.
[8] Liu Y, Lan YF, Zhang H, et al. Optical rotatory power of polymer-stabilized blue phase liquid crystals. Appl Phys Lett. 2013;102:131102.
[9] Choi H, Higuchi H, Kikuchi H. Fast electro-optic switching in liquid crystal blue phase II. Appl Phys Lett. 2011;98:131905.
[10] Kim MS, Chien L-C. Topology-mediated electro-optical behaviour of a wide-temperature liquid crystalline amorphous blue phase. Soft Matter. 2015;11:8013–8018.
[11] Haseba Y, Kikuchi H, Nagamura T, et al. Large electro-optic kerr effect in nanostructured chiral liquid-crystal composites over a wide temperature range. Adv Mater. 2005;17:2311–2315.
[12] Tanabe Y, Furue H, Hatano J. Optically isotropic liquid crystals with microsized domains. Mater Sci Eng: B. 2005;120:41–44.
[13] Benmouna R, Coqueret X, Maschke U, et al. Investigation of Polymer Dispersed Liquid Crystal films exhibiting nanosized liquid crystalline domains. Mol Cryst Liq Cryst. 2004;422:135–141.
[14] Aya S, Le KV, Araoka F, et al. Nanosize-induced optically isotropic nematic phase. Jpn J Appl Phys. 2011;50:051703.
[15] West JL. Phase separation of liquid crystals in polymers. Mol Cryst and Liq Cryst Incorp Nonlinear Opt. 1988;157:427–441.
[16] Justice RS, Schaefer DW, Vaia RA, et al. Interface morphology and phase separation in polymer-dispersed liquid crystal composites. Polymer. 2005;46:4465–4473.
[17] Kang SG, Kim JH. Optically-isotropic nanoencapsulated liquid crystal displays based on Kerr effect. Opt Exp. 2013;21:15719–15727.
[18] Kim N, Kim DY, Park M, et al. Optically isotropic liquid crystal media formulated by doping star-shaped cyclic oligosiloxane liquid crystal surfactants in twin nematic liquid crystals. Soft Matt. 2015;11:3772–3779.
[19] Lim YJ, Kim HJ, Chae YC, et al. Fast switching and low operating vertical alignment liquid crystal display with 3-D polymer network for flexible display. IEEE Trans on Elect Devi. 2017;64:1083–1087.
[20] Drzaic PS. Reorientation dynamics of polymer dispersed nematic liquid crystal films. Liq Cryst. 1988;3:1543–1559.
[21] White TJ, Natarajan LV, Bunning TJ, et al. Contribution of monomer functionality and additives to polymerization kinetics and liquid crystal phase separation in acrylate-based polymer-dispersed liquid crystals (PDLCs). Liq Cryst. 2007;34:1377–1385.
[22] Pogue RT, Natarajan LV, Siwecki SA, et al. Monomer functionality effects in the anisotropic phase separation of liquid crystals. Polymer. 2000;41:733–741.

[23] Deshmukh RR, Malik MK. Effect of temperature on the optical and electro-optical properties of poly (methyl methacrylate)/E7 polymer-dispersed liquid crystal composites. J Appl Poly Sci. 2008;109:627–637.

[24] Cho JD, Lee SS, Park SC, et al. Optimization of LC droplet size and electro-optical properties of acrylate-based polymer-dispersed liquid crystal by controlling photocure rate. J Appl Poly Sci. 2013;130:3098–3104.

[25] Niiyama S, Hirai Y, Kumai H, et al. A hysteresis-less LCPC device for a projection display. SID Digest '92. 1992:575–578.

[26] Park CH, Shin EJ, Manda R, et al. Fast response and scattering free optically isotropic liquid crystal device for flexible display applications. SID Int Symp Dig Tech Pap. 2016;47:1506–1508.

[27] Cho NH, Nayek P, Lee JJ, et al. High-performance, in-plane switching liquid crystal device utilizing an optically isotropic liquid crystal blend of nanostructured liquid crystal droplets in a polymer matrix. Mater Lett. 2015;153:136–139.

[28] Yu JH, Lee JJ, Lim YJ, et al. Optically isotropic polymer dispersed liquid crystal composite for high contrast ratio and fast response time. SID Int Symp Dig Tech Pap. 2013;44:1338–1340.

[29] Yu JH, Chen HS, Chen PJ, et al. Electrically tunable microlens arrays based on polarization-independent optical phase of nano liquid crystal droplets dispersed in polymer matrix. Opt Exp. 2015;23:17337–17344.

[30] Shin EJ, Noh SC, Kim TH, et al. Enhancement of electro-optic properties of optically isotropic liquid crystal device for flexible display. SID Int Symp Dig Tech Pap. 2015;46:1483–1486.

[31] Montgomery GP Jr, West JL, Tamura-Lis W. Light scattering from polymer-dispersed liquid crystal films: droplet size effects. J Appl Phy. 1991;69:1605–1612.

[32] Kerr JXL. A new relation between electricity and light: dielectrified media birefringent. The London, Edinburgh, and Dublin. Philos Mag J Sci. 1875;50:337–348.

[33] Yan J, Rao L, Jiao M, et al. Polymer-stabilized optically isotropic liquid crystals for next generation display and photonics applications. J Mater Chem. 2011;22:7870–7877.